RELATIVE CATALYTIC ACTIVITY OF IRON CONTAINING MINERALS FOR THE HYDROGASIFICATION OF COAL*

Thomas D. Padrick, James K. Rice, and Thomas M. Massis
Sandia National Laboratories, Albuquerque, NM 87185

INTRODUCTION

Hydrogasification of coal is a technique for producing synthetic natural gas (SNG) which offers the advantage of methane production in a single process step. A fundamental limitation of hydrogasification is the low reactivity of hydrogen, compared to steam or oxygen, towards coal chars. Utilization of a low-cost catalyst that would greatly enhance the reactivity of hydrogen towards coal char would significantly impact the SNG program.

It has been known for some time that various inorganic species have a catalytic effect on gasification rates of carbons and graphites (1). Recently, Hüttinger and Krauss (2) investigated the catalytic activity of coal minerals in the hydrogasification of coal. They studied six bituminous coals in a fixed-bed flow reactor at pressures up to 2 MPa and temperatures from 400 to 960°C. Methane formation was observed in three distinct ranges between 500 and 600°C, 750 to 800°C, and >850°C. They determined that in the region >850°C, iron can accelerate methane formation significantly if the pressure is sufficiently high.

We investigated the catalytic activity of several iron compounds on the hydrogasification of a Pittsburgh Seam coal at one atmosphere of H_2 (3). We observed that the catalytic activity is dependent on the particular iron compound with the following order observed (most active to least active): Fe_2O_3 > Fe_3O_4 > $FeSO_4$ > FeS_2 > FeO > Fe. In this paper, we shall describe the results of two series of experiments performed to aid in interpreting this dependence of reduced iron catalytic activity on precursor species. It has been assumed that the role of reduced iron in catalyzing hydrogasification is dissociation of H_2 (4). Also, there is evidence that catalysts affect gasification by physical interaction with the coal (5). Thus, we shall report measurements of the H_2/D_2 exchange activity over reduced iron compounds and present data on surface areas and total pore volumes for chars formed from the coal plus iron compound samples. Finally, we shall discuss these results with respect to the observed dependence of gasification rates on the particular iron compound added.

H_2/D_2 EXCHANGE STUDIES

Experiment and Results

For the H_2/D_2 exchange experiments, the experimental apparatus consisted of a flow controlled source of H_2 and D_2, a gas mixing section, and a temperature controlled oven. The catalyst sample was contained within a 0.5 cm I.D. quartz tube inside the oven. An iron-constantan thermocouple mounted on the wall of the tube was used to monitor the sample temperature.

* This work supported by the U.S. Department of Energy under Contract DE-AC04-76DP00789.

The experimental procedure was as follows. A sample of each iron compound, of sufficient weight to contain 70 mg of elemental iron, was positioned in the quartz tube between quartz-wool plugs. An approximately equimolar flow of H_2 and D_2 was established through the sample at a nominal flow rate of 25 ml/min. The oven temperature was raised to 1000°C and held there for thirty minutes to reduce the sample to elemental iron. Under a continuous steady flow of H_2 and D_2, the sample temperature was lowered to the desired measurement temperature and stabilized there. In-line sample bottles at the entrance and exit of the oven were used to obtain a sample of the H_2/D_2 mixture before its passage through the catalyst and a sample of the $H_2/D_2/HD$ mixture after the catalyst. These gases were then analyzed with a calibrated UTI quadrupole mass spectrometer to determine the HD/H_2 and D_2/H_2 ratios. Blank runs, with H_2/D_2 flow through heated quartz-wool without a catalyst sample, showed no conversion to HD.

The yield of HD in the gas sample collected after passage through the catalyst is plotted as a function of sample temperature in Figures 1 and 2. In plotting these figures, the amount of HD in the sample was divided by the amount of HD that we expected to be present based on thermodynamic equilibrium. These temperature-dependent data show several interesting features. Each sample exhibits a characteristic temperature at which the conversion reaction is catalyzed. For higher temperatures, the HD yield is within a few percent of the thermodynamic value but appears to consistently exceed it. Also, samples that exhibit larger characteristic temperatures also show a more gradual rise in HD yield with increasing temperature, while samples with a low characteristic temperature show a very rapid change to full activity. From Figs. 1 and 2, we can conclude that the relative ordering for catalyzing H_2/D_2 exchange over the reduced iron compounds is $Fe_3O_4 > Fe_2O_3 > Fe > FeO > FeSO_4 > FeS_2$. This ordering assumes that the more active catalysts are the ones with the lower characteristic temperatures.

Model

The results presented above can be interpreted on the basis of a simple phenomenological model, which we derive below. We assume that a fraction of the H_2 and D_2 (and HD when present) flowing through the catalyst are chemisorbed (and dissociated) on the iron surface. The HD can be formed by a variety of gas/surface interaction mechanisms (6). For the present model, we will assume a purely surface mechanism; that is, HD is produced by the association of H and D atoms on the surface and subsequent desorption of HD. For this mechanism, the rate of HD formation is governed by

$$HD + 2S \underset{k_-}{\overset{k_+}{\rightleftharpoons}} S_H + S_D \qquad (1)$$

where S is the concentration of empty, potentially active surface sites and S_H and S_D are the concentrations of surface sites containing H and D atoms, respectively. We assume that the available sites are rapidly occupied by H and D atoms at an equilibrium concentration that is insensitive to the concentration of HD. Denoting these equilibrium concentrations by superscript "e", we obtain from Eq. (1) the following rate equation for HD formation

$$\frac{d\,HD}{dt} = k_{-}\, S_D^e\, S_H^e \left(1 - \frac{HD}{HD^e}\right) \qquad (2)$$

In deriving Eq. (2), we have required the time derivative to vanish as $t \to \infty$ and $HD \to HD^e$. Integrating Eq. (2) over the time interval τ for which the gas stream is in contact with the catalyst yields

$$\frac{HD}{HD^e} = 1 - \exp\left(-\exp\left(\frac{E}{R}\left(\frac{1}{T_o} - \frac{1}{T}\right)\right)\right) \qquad (3)$$

where

$$k_{-} \equiv Ae^{-E/RT}$$

and

$$T_o \equiv \frac{E/R}{\ln\left(\frac{S_D^e\, S_H^e\, A\, \tau}{HD^e}\right)}$$

Equation (3) contains two parameters that characterize the data, a characteristic temperature T_o at which the sample becomes effective in catalyzing the exchange reaction, and an energy E, which represents the overall activation energy associated with the surface reaction of H and D to form desorbed HD.

This model fits the experimental data quite well as shown by the solid lines in Figs. 1 and 2. An E/R value of 15,000 K is assumed for all the data, while T_o is chosen to fit each data set separately. (The value for E/R was chosen to agree with measured adsorption energies of ∿30 Kcal/mole.) The fact that all the data, regardless of the composition of the compound prior to reduction, are well represented by the same value of E indicates that the active sites in all the reduced minerals are energetically similar. However, the widely different values of T_o suggest that the density of active sites (or their accessibility) varies considerably from sample to sample.

Apart from temperature, the only experimentally adjustable parameter in the model is the contact time τ. To check the predictive capability of the model, we increased the contact time by a factor of 25 for H_2/D_2 on reduced FeS_2. This increase was accomplished by slowing the flow rate a factor of 5 to 5 ml/min and increasing the amount of sample by a factor of 5. Such an increase in τ is expected to decrease T_o (see Eq. (3)) from 1073 K to 873 K. As shown by the dashed line in Fig. 2, the data and the model prediction agree reasonably well.

SURFACE AREA STUDIES

Experiment and Results

The analysis of the Pittsburgh seam coal used in these studies is listed in Table 1. This coal was chosen because of its low inherent mineral matter content and high free swelling index. (Addition of minerals is less complicated by inherent minerals, and changes in agglomerating properties are easily observed.) The average particle size of the coal sample used was 15μ with the entire sample passing through a 75μ screen. Mixtures of coal plus minerals were prepared

Table 1. Analysis of the Pittsburgh Seam Coal from the Bruceton Mine

Proximate Analysis	Wt. %
Moisture:	1.47
Ash:	3.80
Volatile:	34.66
Fixed Carbon:	60.07

Ultimate Analysis	Wt. %
Moisture:	1.47
Carbon:	79.43
Hydrogen:	5.13
Nitrogen:	1.67
Chlorine:	0.01
Sulfur:	1.02
Ash:	3.80
Oxygen (diff):	7.47

Sulfur Forms	Wt. %
Pyritic:	0.31
Sulfate:	0.06
Organic (diff):	0.65

Rank	hvAb
Free Swelling Index	7

Petrographic Analysis	Vol. %
Vitrinite:	72.1
Exinite:	7.2
Inertinite:	20.7

by physical mixing unless otherwise indicated. Analysis for sulfur content (for FeS_2) or x-ray fluorescence measurement of iron concentration (for other iron compounds) indicates that for the sample size used in the present experiments, uniform mixtures had been achieved.

Char samples for the surface area and total pore volume measurements were prepared by heating coal samples in a Dupont 951 thermal gravimetric analysis apparatus to 1000°C and then cooling to ambient temperature. For all samples in which an iron compound was added to the coal, the normal agglomerating property of the Bruceton coal was completely destroyed. The char sample, prepared from the raw Bruceton coal, was repulverized before use. (Repulverization of the raw coal char reduced it to a particle size similar to the other chars, but made a negligible contribution to the surface area.) The nitrogen BET (7) surface area and total pore volume for each char was measured on a Micromeritics Digisorb pore-volume/surface area analyzer.

The results from surface area studies on the raw coal char and chars from three samples of coal plus catalyst are listed in Table 2. We found that addition of the iron containing minerals greatly increased the surface area and pore volume of the resulting char. Table 2 also reveals large differences in the size of the increase in surface area, depending on the particular iron compound added. The relative ordering of these physical effects on the coal char is that $FeSO_4$ > Fe_2O_3 > Fe.

DISCUSSION

In our earlier work on mineral matter effects on hydrogasification of coal, we measured gasification rates for samples of Bruceton Mine coal with various iron containing minerals. These results are listed in Table 3. We observed that, although all the minerals used were quickly reduced to elemental iron, the gasification rate was dependent on the particular mineral added. We speculated that this dependence on precursor species was related to active site density in the reduced

Table 2. Nitrogen BET Surface Areas and Total Pore Volumes

Char Source	Surface Area (m^2/g)	Total Pore Volume (cc/g)
Bruceton Coal	3.3	0.0013
Bruceton + 3.5% Fe	10.2	0.0061
Bruceton + 5% Fe_2O_3	48	0.0101
Bruceton + 9.5% $FeSO_4$	90	0.0307

form of each mineral, since all were of similar particle size and samples were prepared to contain the same quantity of reduced iron.

The H_2/D_2 exchange experiment was designed to test the hypothesis that the relative ordering of hydrogasification rates was correlated to the active site density. We see from the results given above that different iron containing minerals, when reduced, yield varying active site densities for hydrogen exchange. However, the relative ordering for hydrogen exchange is not the same as the observed relative ordering for hydrogasification rates. Thus, active site density alone cannot explain the relative ordering of hydrogasification rates.

Results given above for surface areas on three samples also show that the iron compounds affect the chars differently. If we assume that an increase in surface area and a more open pore structure enhance the gasification rate of a char, then we would expect a change in gasification rates from this physical effect. However, the relative ordering of surface areas is not the same as the observed relative ordering for hydrogasification rates. Hence, physical changes alone in the char cannot explain the measured hydrogasification rates.

For the three samples that we have investigated thus far, it appears that a combination of hydrogen transfer activity and physical effect

Table 3. Gasification Rates of Bruceton Mine Coal at 1000°C in H_2 with Various Iron Compounds

Sample	$\frac{dw}{dt}$ (mg/min)
Raw Coal	2.1×10^{-3}
Coal + 3.5% Fe (3μ)	5.2×10^{-3}
Coal + 7% FeS_2 (5μ)	1.0×10^{-2}
Coal + 5% Fe_3O_4 (5μ)	2.5×10^{-2}
Coal + 5% Fe_2O_3 (5μ)	4.0×10^{-2}
Coal + 9.5% $FeSO_4$	2.2×10^{-2}
Coal + 4.5% FeO (5μ)	6.3×10^{-3}

on the char could explain the observed hydrogasification rates. The weighting factors for each of the two effects have not been determined. We will attempt to determine these factors after BET surface area and pore volume data are obtained on the remaining samples.

CONCLUSION

We have measured the hydrogen transfer activity of the reduced iron state for six iron containing minerals. We observed that each mineral resulted in a different active site density. We also measured the nitrogen BET surface area and total pore volume on coal char samples with added iron containing minerals. Again, we observed that each mineral affected the physical structure of the char differently. We have concluded that the catalytic activity of iron containing minerals for the hydrogasification of coal is related both to the hydrogen transfer active site density in the reduced iron state of each mineral and to the physical effect each mineral has on increasing the surface area and pore volume of the devolatilized coal char.

REFERENCES

1. P. L. Walker, Jr., M. Shelef and R. A. Anderson in "Chemistry and Physics of Carbon" (Ed., P. L. Walker, Jr.) Vol. 4, Marcel Dekker, New York, 1968, pp. 287-380.

2. K. J. Hüttinger and W. Krauss, Fuel 60, 93 (1981).

3. T. D. Padrick, D. D. Dees, and T. M. Massis, 11th North American Thermal Analysis Society Conference Proceedings, New Orleans, LA, October (198k), pp. 401-408.

4. A. Tomita, O. P. Mahajan, and P. L. Walker, Jr., Preprints, Amer. Chem. Soc., Div. of Fuel Chem., 24 (3), 10 (1979).

5. S. P. Chauhan, H. F. Feldmann, E. P. Stambaug, and J. H. Oxley, Preprints, Amer. Chem. Soc., Div. of Fuel Chem., 22 (1), 38 (1977).

6. See, for example, J. C. Cavalier and E. Chorust, Surface Science 60, 125 (1976).

7. Based on equations given by S. Brunnauer, P. H. Emmett, and E. Teller, J. Amer. Chem. Soc. 60, 309 (1938).

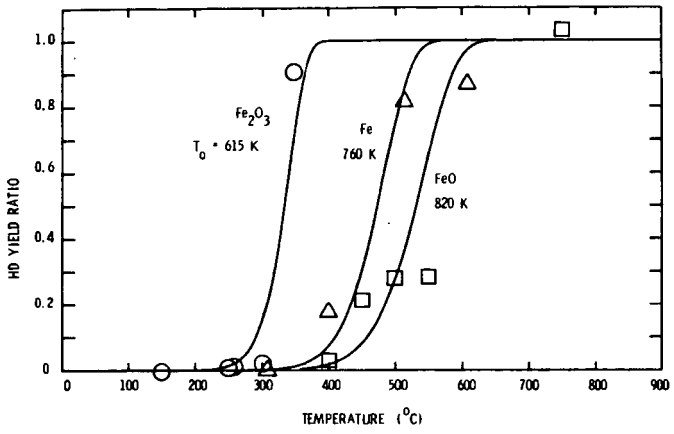

Figure 1. The HD-yield ratio, defined as the amount of HD in the gas sample after passage through the catalyst divided by the amount to be expected at thermodynamic equilibrium, as a function of temperature. The solid lines are calculated from Eq. (3) with E/R = 15,000 K and the indicated value of T_0. The data are represented by symbols: Fe_2O_3 by circles, Fe by triangles, and FeO by squares.

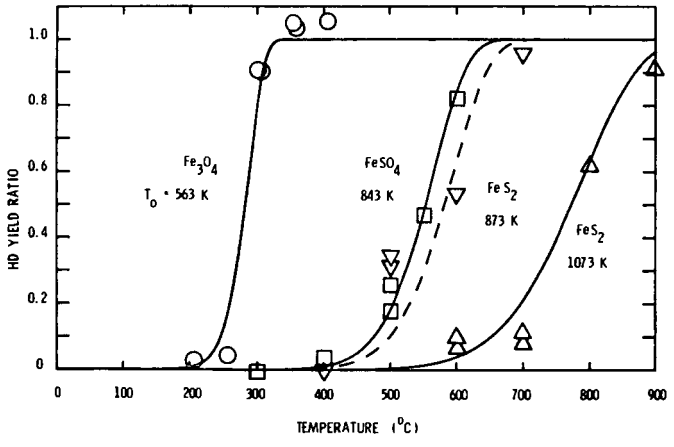

Figure 2. Same as Figure 1, except that data for Fe_3O_4 (circles), $FeSO_4$ (squares), and FeS_2 (triangles and inverted triangles) are represented. The significance of the dashed line is explained in the text.